Available online at www.sciencedirect.com
SCIENCE DIRECT®
International Journal of Heat and Mass Transfer 48 (2005) 3454–3460
International Journal of HEAT and MASS TRANSFER
www.elsevier.com/locate/ijhmt

Note on the mechanism of interfacial mass transfer of absorption processes

Youguang Ma [a,*], Guocong Yu [a], Huai Z. Li [b]

[a] School of Chemical Engineering and Technology, State Key Laboratory of Chemical Engineering, Tianjin University, Tianjin 300072, PR China
[b] Laboratoire des Science du Génie Chimique, CNRS-ENSIC-INPL, 1 rue Grandville, BP 451, 54001 Nancy Cedex, France

Received 23 April 2004

Abstract

A concept that the driving force of gas–liquid interphase mass transfer comes from the interfacial non-equilibrium is proposed in this paper. For the absorption process, based on the general chemical potential driving force equation, the concentration relation between two phases at interface is derived and solved under different conditions as mass transfer occurs, it shows that the interfacial concentration of absorbed component at liquid side is strongly affected by a Biot number Y_0 and is bulk concentration dependent. The CO_2 interfacial concentration of liquid side in stationary absorption by pure methanol, ethanol and *n*-propanol absorbent respectively are measured by the use of micro laser holographic interference technique, the experimental results are in good agreement with the computation.

Keywords: Interfacial non-equilibrium; Laser holographic interference; Gas–liquid interphase mass transfer; Interfacial concentration

1. Introduction

Gas–liquid interphase mass transfer is widely encountered in many industrial fields such as chemical, refinery, biochemical, pharmaceutical and environment protection etc. Some unit operation processes like absorption, distillation and desorption involve typically gas–liquid two phase mass transfer, which is also of key importance in gas–liquid two phase fluid reactor. Film model [1], penetration theory [2] and surface renewal model [3] are three classical and well-known theories describing interphase mass transfer and have been extensively used in practical processes. On the basis of these models, film-penetration model [4] and eddy cell model [5] were further developed in terms of turbulent theory. Levich [6] and Lochiel and Calderbank [7] have solved the convection–diffusion equation according to the fluid field characteristic near the interface and obtained the concentration distribution close to the interface which finally leads to the solution of mass transfer coefficient. Among all these models proposed, film model received the most attention due to its simplicity and accuracy comparable with other models, particularly the concept of resistance sum has been generally accepted and adopted [8–12]. In fact, an assumption that the gas and liquid phases are in thermodynamic equilibrium at interface during the process of mass transfer has to be used to derive these models above because of both the limitation of experimental instrumentation and theoretical difficulty. Although equilibrium assumption simplified the solution

* Corresponding author. Tel.: +86 22 27403584; fax: +86 22 27404757.
E-mail address: ygma@tju.edu.cn (Y. Ma).

0017-9310/$ - see front matter © 2005 Elsevier Ltd. All rights reserved.
doi:10.1016/j.ijheatmasstransfer.2005.03.008

Nomenclature

C	total molar concentration, mol cm^{-3}
d_e	equivalent bubble diameter, cm
D	diffusivity in Fick's equation, cm^2 s^{-1}
D'	diffusivity in Maxwell–Stefan equation, cm^2 s^{-1}
H	shifting distance of stripe, cm
J	diffusion flux, mol cm^{-2} s^{-1}
k_l	rate coefficient of mass transfer in liquid side, cm^2 s^{-1}
l	thickness of simulator, cm
n	refraction index
R	universal gas constant, J mol^{-1} K^{-1}
S	interval between two neighboring stripes, cm
T	absolute temperature, K
u	liquid flow velocity, cm^2 s^{-1}
x	molar fraction of solute at interface
x^*	equilibrium molar fraction of liquid solute with gas at interface
Y_0	Biot number

Greek symbols

λ	wavelength of laser, cm
γ	activity coefficient of solvent in solution
δ	thickness of concentration boundary layer in liquid side, cm
μ	chemical potential, J mol^{-1}

Subscripts

cal	calculated value
exp	experimental value
A	component A
B	component B
b	bulk liquid
g	gas phase
l	liquid phase

of problem, it is harmful to the understanding of the process mechanism by neglecting the influence of interface itself and source of driving force for interphase mass transfer. Up to now, all existing theories of mass transfer are only of limited application and there is no ad hoc model permitting to precisely elucidate the mechanism of interfacial mass transfer. In recent years, due to the exponentially expanding power of computer, increasing emphasis has been paid to the micro mechanism model being of little deviation and able to be used under various operating conditions, moreover, advanced laser measurement techniques are also capable of supplying some helpful underlying qualitative and quantitative information to establish mechanism models [13,14]. This paper aims at investigating the influence of interface on interphase mass transfer and exploring the micro mechanism on the basis of existing theories.

2. Theory

Interfacial resistance has been early found in the evaporation of a pure liquid [15], Cable and Cardew [16] studied the kinetics of desorption with interfacial resistance. Gupta and Sridhar [17] investigated the influence of interfacial resistance on quiescent gas–liquid absorption. In fact, because of the lack of experimental accuracy about the existence of interfacial resistance in gas–liquid or liquid–liquid mass transfer, which is usually considered resulting from interfacial or surface contamination due to surfactants [18], consequently much attention has been paid to the experimental investigation and theoretical description for the effect of surfactant on interphase mass transfer [19–25]. However, a few authors proposed the interfacial non-equilibrium during interphase mass transfer [11,26,27]. The authors of the present paper think that for a gas–liquid or a liquid–liquid mass transfer system, the equilibrium of the driving force must be maintained in the overall system; the chemical potential difference between two phases at the interface is a potential energy to force mass transfer. The mathematical model is derived below under this consideration.

Fick's law is a fundamental flux equation corresponding to the concentration driving force mass transfer

$$J_A = -D_{AB}\frac{dC_A}{dy} \tag{1}$$

where D_{AB} is diffusivity.

In momentum transfer the sheer stress approaches zero as the velocity gradient decreases, and the two phases reach a thermal equilibrium when the temperature becomes equal. Thus it is logical and more reasonable to assume that the chemical potential of each component becomes equal throughout the system [28]

$$J_A = -\frac{D'_{AB}C_A}{RT}\frac{d\mu_A}{dy} \tag{2}$$

where D'_{AB} is a diffusivity corresponding to the driving force of chemical potential defined by the equation above which states that the flux is proportional to the gradient of chemical potential, these two diffusivities can be related by the equation

$$D_{AB} = D'_{AB}\left(1 + x_2 \frac{\partial \ln \gamma_2}{\partial x_2}\right) \tag{3}$$

For a system of ideal solution

$$D_{AB} = D'_{AB} \tag{4}$$

Taking into account an absorption process of ideal system with an assumption that the resistance in gas side is negligible and the resistance in liquid side to mass transfer by driving force of chemical potential exists only in a thin film—concentration boundary layer adjacent to the interface, Eq. (2) can be rewritten by integral

$$\Delta\mu = -\frac{J_A RT\delta}{D_{AB}C_A} \tag{5}$$

where C_A is considered as a constant

$$C_A = \frac{C_I + C_b}{2} \tag{6}$$

The difference of chemical potential between gas and liquid phases at interface can be calculated in terms of molecular thermodynamics [29]

$$\Delta\mu = -(\mu_{g,I} - \mu_{l,I}) = -RT \ln \frac{x^*}{x_I} \tag{7}$$

The chemical potential difference is the more plausible driving force of mass transfer between two phases, combining Eqs. (5)–(7), we have

$$\ln \frac{x^*}{x_I} = \frac{2J_A\delta}{D_{AB}(C_I + C_b)} \tag{8}$$

The flux expressing equation based on the driving force of concentration difference is

$$J_A = k_l(C_I - C_b) \tag{9}$$

Comparing Eqs. (8) with (9), we have

$$\ln \frac{x^*}{x_I} = \frac{2k_l\delta(C_I - C_b)}{D_{AB}(C_I + C_b)} = \frac{2k_l\delta(x_I - x_b)}{D_{AB}(x_I + x_b)} \tag{10}$$

It is convenient to define a Biot number Y_0 as

$$Y_0 = \frac{k_l\delta}{D_{AB}} \tag{11}$$

It can be found easily that Y_0 number shows the deviation of practical operation to film model in mass transfer coefficient, which is a function depending on material properties and operation state, substituting Y_0 to Eq. (10) and further writing as

$$\frac{x^*}{x_I} = e^{\frac{2Y_0(x_I - x_b)}{x_I + x_b}} \tag{12}$$

For the case of following film model, $Y_0 = 1$, we have

$$\frac{x^*}{x_I} = e^{\frac{2(x_I - x_b)}{x_I + x_b}} \tag{13}$$

By Eq. (13) the real concentration at interface during mass transfer between two phases can be obtained. Table 1 gives the interfacial concentration under different liquid bulk concentrations. In order to compare the resistance on liquid side with that at interface, defining an interfacial mass transfer coefficient by the equation

$$J_A = k_I(C^* - C_I) \tag{14}$$

Interfacial resistance of mass transfer is given by

$$R_I = \frac{1}{k_I} \tag{15}$$

Comparing to the resistance of mass transfer in liquid side, we have

$$\frac{R_I}{R_l} = \frac{x^* - x_I}{x_I - x_b} \tag{16}$$

Table 1 shows that the interfacial concentration is far from the equilibrium value as mass transfer occurs, there exists a larger deviation for smaller liquid bulk concentration. The difference $\frac{x_I}{x^*} - \frac{x_b}{x^*}$ represents the real concentration driving force in liquid side. For the system in which the film model is approximately tenable, the practical driving power for mass transfer comes to the maximum when liquid dimensionless concentration $\frac{x_b}{x^*}$ is in the range of 0.2–0.3. Comparing with the resistance of mass transfer in liquid side, the interfacial resistance is of much larger value, in this situation, the assumption of equilibrium is not justifiable. In fact, dimensionless number Y_0 is strongly dependent on both system and operating condition. As a prerequisite that the Y_0 will have to be primarily achieved by solving the convection–diffusion equation of fluid in motion with the resorting to turbulent theory in order to obtain real interfacial concentration and finally get mass transfer

Table 1
The calculating results of interfacial concentration

$\frac{x_b}{x^*}$	0	0.1	0.2	0.3	0.4	0.5	0.6	0.7	0.8	0.9	1.0
$\frac{x_I}{x^*}$	0.1353	0.3375	0.4572	0.5527	0.6350	0.7083	0.7751	0.8368	0.8945	0.9487	1.0
$\frac{x_I}{x^*} - \frac{x_b}{x^*}$	0.1353	0.2375	0.2572	0.2527	0.2350	0.2083	0.1751	0.1368	0.0945	0.0487	1.0
$\frac{R_I}{R_l}$	6.39	2.79	2.11	1.76	1.55	1.40	1.28	1.19	1.12	1.05	

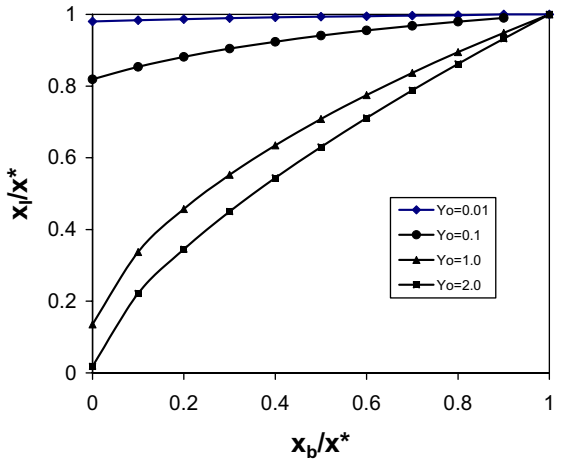

Fig. 1. The variation of interfacial concentration with liquid bulk concentration under various Y_0 conditions.

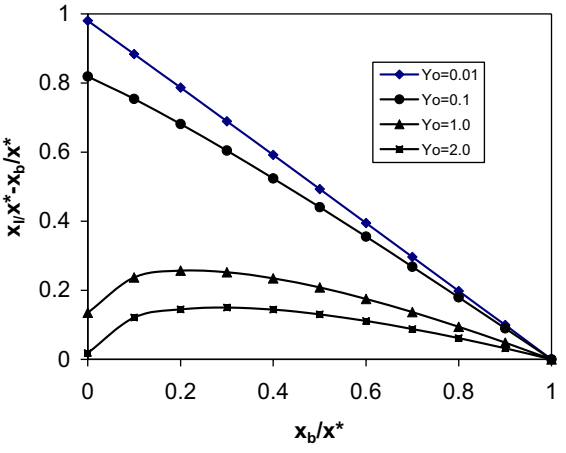

Fig. 2. The influence of liquid bulk concentration on concentration driving force in liquid side under various Y_0 conditions.

flux. Some special solution can be obtained according to various operation conditions.

Figs. 1 and 2 indicate respectively the variation of interfacial concentration with liquid bulk concentration under various Y_0 conditions.

3. Experiment

In recent decades, the laser measurement techniques have been prevalently applied to precise qualitative and quantitative measurement of diverse parameters in fluid like velocity, temperature, concentration and density etc. with the advantages of high accuracy, non-intrusive and feasibility to make instantaneous measurement and visualization. However, it is still quite difficult to perform the measurement of concentration change in a slower-rate and very smaller-amount physical absorption process due to little concentration variation which is insensitive to refraction index by means of the simple and ordinary optical methods of interference. In this paper, the real-time method [14] and micro laser holographic interference technique were used for the determination of concentration field and its variation near the interface on liquid side during absorption process. In the first exposure, the comparison wave is recorded, and the hologram developed, fixed and repositioned accurately into the plate holder. The comparison wave is reconstructed by illuminating the hologram with the reference wave. The reconstructed wave can be superimposed to the momentary object wave. If the object wave corresponds to the original state in which the hologram is taken, no interference fringes appear. When the mass transfer process is started, the resulting object wave is distorted, and behind the hologram, the object wave and the reference wave interfere and form an interference pattern which can be observed continuously and also filmed or photographed. In our experiments, a special single source laser holographic interferometer with optical magnification which is essential to gain a satisfactory view of interference fringes within the thin concentration boundary layer has been constructed for the study of gas absorption by a pure absorbent as shown in Fig. 3. The laser beam from a He–Ne laser source is splitted into two coherent beams, one (objective beam) passes through the bubbling simulator at a point near the interface of a rising bubble, while the other (reference beam) bypasses the simulator. These two beams intersect at the photographic plate to form a hologram by interference. The two beam amplifying lens 6 and 9 should be carefully chosen and adjusted to hologram. In addition, to obtain more exact information, a parallel vertical and suitable interval of fringes are formed

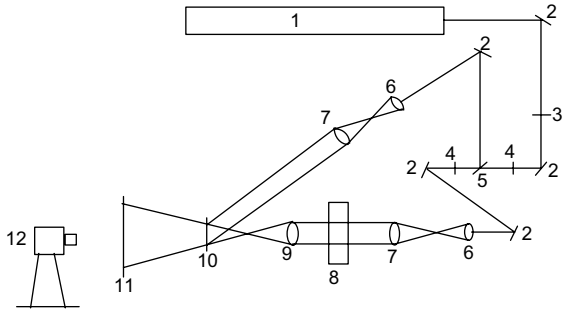

Fig. 3. Optical representation of single source laser interferometer: 1—He–Ne laser, 2—mirrors, 3—shutter, 4—polarisation filters, 5—beam-splitter, 6—spatial filters, 7—lenses, 8—simulator, 9—amplifying lens, 10—holographic plate, 11—frosted glass, 12—camera.

artificially and preveniently by micro adjusting the optical unit in the optical path. As no concentration changed, the stripes are parallel and vertical to interface with same interval. Whereas if concentration changed, the stripes would shift simultaneously. For arbitrary two points $A(x_0, y_0)$ referring to bulk concentration and $B(x, y)$ responding to changed concentration as shown in Fig. 4, has

$$n = n_0 - \frac{H\lambda}{lS} \tag{17}$$

where n is the refraction index in point $B(x, y)$, n_0 the refraction index of bulk in point $A(x_0, y_0)$, H the shifting of stripe $(y - y_0)$, l the thickness of simulator, λ the wavelength of laser, and S the interval between two neighboring stripes. The relation of concentration to refraction index is determined experimentally and fitted.

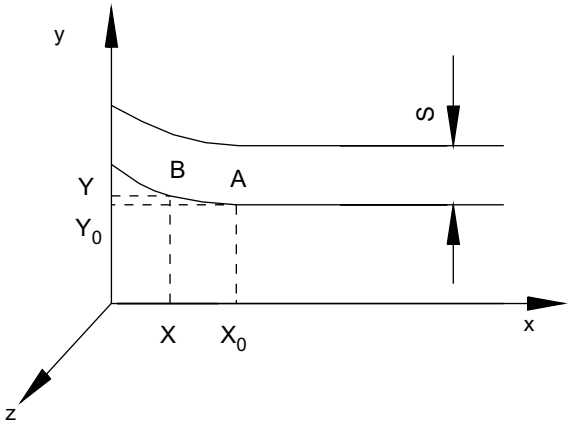

Fig. 4. Schematic diagram of the interference stripes variation.

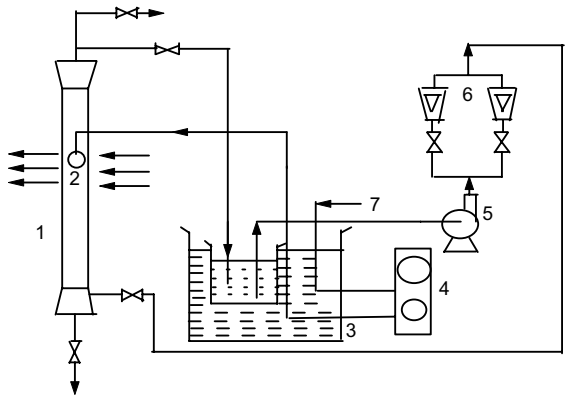

Fig. 5. Schematic flowshow of experimental set-up: 1—bubbling simulator, 2—captured bubble, 3—thermostat, 4—controller, 5—pump, 6—flow meter, 7—injector.

Fig. 5 is the schematic diagram of gas–liquid flowing simulator. The liquid was pumped to the top of a vertical rectangular channel 1 in optical glass, and flowed downward to the bottom. The incoming liquid was introduced through a horizontal perforated tube to ensure uniform distribution. The gas phase was injected into the channel by syringe 7 and the bubble size was carefully controlled by the injection-flowrate. A small metal mesh was installed in the channel to keep the rising bubble in stationary position against the downward current of liquid. By means of thermostat 3, the gas and liquid phases were kept at the same temperature. Figs. 6–8 show the shifts of interference fringes in hologram as CO_2 is absorbed by static and pure absorbent methanol, ethanol, and *n*-propanol respectively under experimental condition. The straight lines in hologram indicate the reference infringes representing the condition of uniform concentration maintained in the bulk fluid, whereas the curved lines illustrate the reference infringes of concentration change induced by mass transfer.

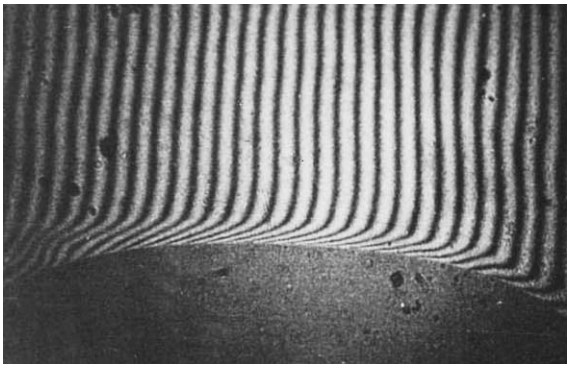

Fig. 6. The hologram of CO_2 absorbed by static methanol.

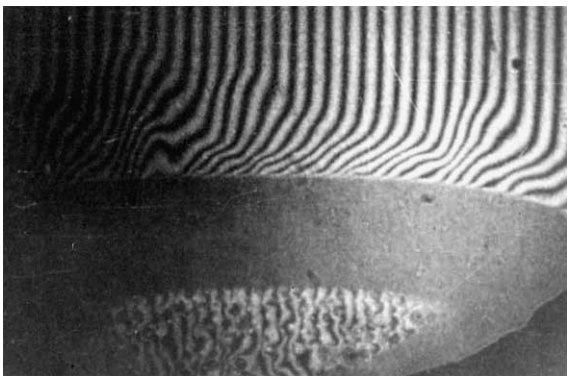

Fig. 7. The hologram of CO_2 absorbed by static ethanol.

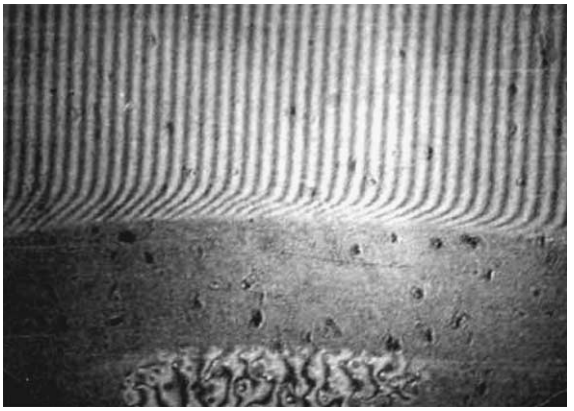

Fig. 8. The hologram of CO_2 absorbed by static *n*-propanol.

4. Results and discussions

An experiment of CO_2 single bubble absorption was carried out. The solvents used in experiments are methanol (99.5 wt.%), ethanol (99.7 wt.%) and *n*-propanol (99.5 wt.%). The concentration of CO_2 is 99.99 (wt.%). The experimental conditions are: $T = 298.15$ K, $P = 101.325$ kPa, and the equivalent bubble diameter $d_e = 0.42$ cm. For a system of pure gas, the resistance of gas film can be neglected, thus the liquid equilibrium concentration at interface is the saturated absorption concentration at the same temperature and pressure. The liquid diffusivities and equilibrium molar fraction of CO_2 in absorbent under experimental condition are respectively: methanol: $D = 3.75 \times 10^{-5}$ cm^2 s^{-1}, $x_2^* = 6.28 \times 10^{-3}$; ethanol: $D = 4.0 \times 10^{-5}$ cm^2 s^{-1}, $x_2^* = 7.15 \times 10^{-3}$; *n*-propanol: $D = 2.79 \times 10^{-5}$ cm^2 s^{-1}, $x_2^* = 8.33 \times 10^{-3}$.

The iterative method is used to calculate the interfacial concentration of CO_2 absorbed by clean solvent. The film model is applied to the static absorption process, thus x_b is zero and Y_0 becomes unit in Eq. (12). As a result, x_I can be solved in terms of Eq. (12) through iterative way with a given initial value between zero and x^*. Table 2 shows the differences of equilibrium, experimental and computed interfacial concentration and their comparison in CO_2 stationary absorption with different pure absorbent. It is apparently found that the interfacial concentrations measured are far from the equilibrium ones and in good agreement with calculated ones. A possible reason for lower calculated values is that the computation based on the film model with $Y_0 = 1$ shifts the practical process in which the mass transfer coefficient is less than that obtained by film model and $Y_0 < 1$.

Table 2
The comparison of experimental, calculating and equilibrium CO_2 interfacial concentrations

Nom	Methanol	Ethanol	*n*-Propanol
$x_{I,cal} \times 10^3$	0.85	0.967	1.13
$x_{I,exp} \times 10^3$	0.992	1.76	1.94
$x^* \times 10^3$	6.28	7.15	8.33

In the literature, widespread attention has been focused on the mass transfer accompanied interfacial turbulence [30–33]. In our works, the visualization of interfacial turbulence is carried out. A drastic turbulence is observed in ethanol absorption, whereas only slight fluctuation is found in methanol and *n*-propanol absorption. The disorder of interference strips near the interface implies the concentration chaos caused by interfacial turbulence as mass transfer occurs. In addition, the experimental observation demonstrates the fact that the processes of interphase mass transfer could be accompanied with strongly or weekly interfacial turbulence. Under low fluid flow velocity and stationary situation, interfacial turbulence is usually initiated at some point of field, resulting from the non-uniformity of mass transfer at interface. This decelerates and comes soon to a stabilization with the increasing liquid flow velocity.

5. Conclusion

In the processes of gas–liquid mass transfer, the two parts outside interface is not at thermodynamic equilibrium arising from the interphase mass transfer. For the system in which the film model is approximately right, the flux is affected comprehensively by material properties, operation condition and liquid bulk concentration. Under the same material properties and operating condition, the rate of interphase mass transfer attains a maximum for a dimensionless bulk concentration ranging from 0.2 to 0.3. A Biot number Y_0 number which shows the deviation of practical mass transfer to that of film model is proposed in this paper, a bigger Y_0 number bring about a larger deceleration from equilibrium. In the situation of model film, $Y_0 = 1$, under other situations, Y_0 could be obtained by solving the convection–diffusion equation of species combining with turbulent theory and dynamical boundary condition. Practically, only in the system of little Y_0 number the assumption of equilibrium at interface is plausibly justified, for instance, as Y_0 is less than 0.5. For a process of gas absorption, when the liquid mass transfer coefficient is used to flux equation, the concentration driving force is $(C_I - C_b)$ instead of $(C^* - C_b)$. The flux of mass transfer is integrally influenced by both the mass transfer coefficient and interfacial concentration. It is just the reason that the flux of interphase mass transfer is not linearly varied with the increasing of mass transfer coefficient. The CO_2 interfacial concentration of liquid side in stationary absorption by pure methanol, ethanol

and *n*-propanol absorbent respectively were measured by the use of micro laser holographic interference technique, the experimental results are in good agreement with calculated ones from the equation proposed. The achievement of this paper is also helpful to the studies of some analogous processes such as distillation, extraction and desorption, bubble nucleation and heat transfer etc.

Acknowledgements

The authors acknowledge the financial support of the National Natural Science Foundation of China (no. 20176036). Ma Youguang wishes to appreciate the aid of China Scholarship Council and Laboratoire des Science du Génie Chimique, CNRS of France during work in France as visiting scholar.

References

[1] W.G. Whitman, The two-film theory of gas absorption, Chem. Metall. Eng. 29 (4) (1923) 146–148.
[2] R. Higbie, The rate of absorption of a pure gas into a still liquid during short periods of exposure, Trans. Am. Inst. Chem. Eng. 31 (1935) 365–377.
[3] P.V. Danckwerts, Significance of liquid-film coefficients in gas absorption, Ind. Eng. Chem. 43 (6) (1951) 1460–1467.
[4] H.L. Toor, J.M. Marchello, Film-penetration model for mass and heat transfer, A.I.Ch.E. J. 4 (1) (1958) 97–101.
[5] J.C. Lamont, D.S. Scott, An eddy cell model of mass transfer into the surface of a turbulent liquid, A.I.Ch.E. J. 16 (4) (1970) 513–519.
[6] V.G. Levich, Physicochemical Hydrodynamics, Prentice-Hall, New York, 1962.
[7] A.C. Lochiel, P.H. Calderbank, Mass transfer in the continuous phase around axisymmetric bodies of revolution, Chem. Eng. Sci. 19 (7) (1964) 471–484.
[8] J. Petera, L.R. Weatherley, Modelling of mass transfer from falling droplets, Chem. Eng. Sci. 56 (16) (2001) 4929–4947.
[9] P. Tom, Oxygen absorption into moving water and tensile solutions, Water Res. 34 (9) (2000) 2569–2581.
[10] A.R. Khan, G. Dimitrios, A.K. Nicholas, K. George, Flux of gases across the air–water interface studied by reversed-flow gas chromatography, J. Chromatogr. A 934 (1–2) (2001) 31–49.
[11] K. Terasaka, J. Oka, H. Tsuge, Ammonia absorption from a bubble expanding at a submerged orifice into water, Chem. Eng. Sci. 57 (18) (2002) 3757–3765.
[12] H. Ernst, M. Jørgen, Application of the two-film theory to the determination of mass transfer coefficients for bovine serum albumin on anion-exchange columns, J. Chromatogr. A 827 (2) (1998) 259–267.
[13] Y.G. Ma, H. Cheng, K.T. Yu, Measurement of concentration fields near the interface of a rising bubble by holographic interference technique, Chin. J. Chem. Eng. 7 (4) (1999) 363–367.
[14] A.S. Mujumdar, R.A. Mashelkar, Advances in Transport Processes VIII, Elsevier, Amsterdam, 1992, pp. 1–58.
[15] W.J. Heideger, M. Boudart, Interfacial resistance to evaporation, Chem. Eng. Sci. 17 (1) (1962) 1–10.
[16] M. Cable, G.E. Cardew, The kinetics of desorption with an interfacial resistance and concentration-dependent diffusivity, Chem. Eng. Sci. 32 (5) (1977) 535–541.
[17] R.K. Gupta, T. Sridhar, Effect of interfacial resistance on quiscent gas–liquid absorption, Chem. Eng. Sci. 39 (3) (1984) 471–477.
[18] J.T. Davies, Turbulence Phenomena, Academic Press, New York, 1972, pp. 69–73.
[19] F.H. Garner, A.R. Hale, The effect of surface active agents in liquid extraction processes, Chem. Eng. Sci. 2 (4) (1953) 157–163.
[20] E.J. Cullen, J.F. Davidson, The effect of surface active agents on the rate of absorption of carbon dioxide by water, Chem. Eng. Sci. 6 (2) (1956) 49–56.
[21] G. Boye-Christensen, S.G. Terjesen, On the action of surface active agents on mass transfer in liquid–liquid extraction, Chem. Eng. Sci. 9 (4) (1959) 225–241.
[22] G. Boye-Christensen, S.G. Terjesen, On the mechanism of interfacial resistance to mass transfer in liquid–liquid extraction, Chem. Eng. Sci. 7 (4) (1958) 222–228.
[23] E. Ruckenstein, Effect of surface active agents on the mass transfer in falling liquid films, Chem. Eng. Sci. 20 (9) (1965) 853–856.
[24] M.E. Weber, The effect of surface active agents on mass transfer from spherical cap bubbles, Chem. Eng. Sci. 30 (12) (1975) 1507–1510.
[25] L. Mekasut, J. Molinier, H. Angelino, Effects of surface-active agents on mass transfer inside drops, Chem. Eng. Sci. 34 (2) (1979) 217–224.
[26] T.K. Sherwood, R.L. Pigford, C.R. Wilke, Mass Transfer, McGraw-Hill, New York, 1975, pp. 181–191.
[27] R.W. Schrage, A Theoretical Study of Interphase Mass Transfer, Columbia University, New York, 1953.
[28] C.O. Bennett, J.E. Myers, Momentum, Heat and Mass Transfer, third ed., McGraw-Hill Book Company, New York, 1982, pp. 495–498.
[29] R.A. Pierotti, The solubility of gases in liquids, J. Phys. Chem. 67 (9) (1963) 1840–1846.
[30] A.A. Golovin, Mass transfer under interfacial turbulence: kinetic regulates, Chem. Eng. Sci. 47 (8) (1992) 2069–2080.
[31] K.R. Semkov, N. Kolev, On the evaluation of the interfacial turbulence (the Marangoni effect) in gas (vapour)–liquid mass transfer: Part I. A method for estimating the interfacial turbulence effect, Chem. Eng. Process. 29 (2) (1991) 77–82.
[32] N. Kolev, K.R. Semkov, On the evaluation of the interfacial turbulence (the Marangoni effect) in gas (vapour)–liquid mass transfer: Part II. A method for estimating the interfacial turbulence effect, Chem. Eng. Process. 29 (2) (1991) 83–91.
[33] E. Sada, H. Kumazawa, M.A. Butt, Absorption of carbon dioxide into aqueous solutions of ethylenediamine: effect of interfacial turbulence, Chem. Eng. J. 13 (3) (1977) 213–217.